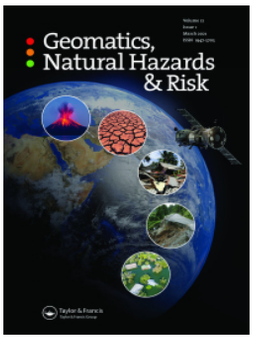

Geomatics, Natural Hazards and Risk

ISSN: 1947-5705 (Print) 1947-5713 (Online) Journal homepage: www.tandfonline.com/journals/tgnh20

Comprehensive assessment of Himalayan glacial lakes concerning their distribution, dynamics, and hazard potential

Litan Mohanty & Prateek Gantayat

To cite this article: Litan Mohanty & Prateek Gantayat (2026) Comprehensive assessment of Himalayan glacial lakes concerning their distribution, dynamics, and hazard potential, Geomatics, Natural Hazards and Risk, 17:1, 2639085, DOI: 10.1080/19475705.2026.2639085

To link to this article: https://doi.org/10.1080/19475705.2026.2639085

GEOMATICS, NATURAL HAZARDS AND RISK
2026, VOL. 17, NO. 1, 2639085
https://doi.org/10.1080/19475705.2026.2639085

Taylor & Francis
Taylor & Francis Group

RESEARCH ARTICLE

OPEN ACCESS Check for updates

Comprehensive assessment of Himalayan glacial lakes concerning their distribution, dynamics, and hazard potential

Litan Mohanty[a,b] and Prateek Gantayat[c]

[a]Department of Himalayan Cryosphere, Wadia Institute of Himalayan Geology, Dehradun, India; [b]Department of Geoscience Division, National Centre for Polar and Ocean Research, Goa, India; [c]Institute of Science and Technology Austria, Klosterneuburg, Austria

ABSTRACT

This study examines the distribution, growth, and GLOF hazard of glacial lakes across major Himalayan river basins. Basin-wise GLOF susceptibility was assessed using glacial lake abundance, spatial distribution, and rates of lake area expansion. The Kosi, Yarlung Zangbo, Manas, and Upper Indus basins were identified as the most susceptible and classified as critical. The highest rates of lake size increase were observed in the Kosi Basin, followed by Yarlung Zangbo, Manas, Karnali, Upper Indus, and Tista, indicating their potential as future GLOF-prone regions. Moreover, a Himalayan-scale GLOF hazard map was generated integrating population, hydropower infrastructure, potential flood volume, roads, settlements, and railways revealing high hazard levels in the Chenab, Jhelum, Teesta, and Beas basins in India; the Koshi, Tama-Koshi, and Dudh-Koshi basins in Nepal; and the Kuri Chu sub-basin of the Manas Basin in Bhutan. These findings highlight priority regions where detailed field investigations and hydrodynamic modelling are essential before further infrastructure development.

ARTICLE HISTORY
Received 21 April 2025
Accepted 20 February 2026

KEYWORDS
Glacial lake; hazard; GLOF; Himalaya; inventory

1. Introduction

Glacial lakes are water bodies present in and around periglacial environments (Quincey 2007, Komori et al. 2012, Zhang et al. 2023). Ample evidence indicates that changes in temperature and precipitation trends significantly impact the formation and expansion of glacial lakes (Mondal et al. 2023). The earliest inventories of glacial lakes identified more than 300 glacial lakes in high mountain Asia (HMA) between 1966 and 1975 (Nikitin 1987). While recent studies by Mohanty et al. (2023a) and Zhang (2023) identified 9280 and 8357 glacial lakes in the Himalayas in 2020, respectively, which shows a large percentage rise in the number of lakes in the Himalayas during the last 50 years.

The high sensitivity of glaciers to global climate change has led to unprecedented retreat of glaciers (e.g. Pelto and Network 2020). This is particularly evident in the Himalayas, where the retreat-led growth of glacial lakes is increasing the risk of GLOFs in the downstream river basins (Bolch et al. 2008, Fujita 2013, Furian et al. 2021). Over the last 30 years, the lakes have expanded by 26% and 30%, according to reports by Mohanty et al. (2023a) and Zhang et al. (2015), with the most significant expansion observed in the eastern and central Himalaya. Although the inventories cannot be directly compared due to differences in methodology, objectives and timeframes, they nonetheless indicate a conservative increase in the number of lakes in the region over time. New glacial lakes are forming at higher elevations along with upglacial expansion of existing lakes (Mohanty and Maiti 2021a; Mohanty et al. 2023a). A total of 1052 new lakes have formed after 1990 (Zhang 2023).

In recent years, the availability of high-quality satellite imagery with improved spatial and spectral resolution has significantly advanced glaciological research, particularly in the areas of glacial lake identification, glacial lake outburst flood (GLOF) event detection, supraglacial debris mapping, geodetic mass balance and glacial lake area change analysis (e.g. Wangchuk and Bolch 2020, Shugar 2021). During

CONTACT Litan Mohanty mohanty.litan.geo@gmail.com
Supplemental data for this article can be accessed online at https://doi.org/10.1080/19475705.2026.2639085.
This article has been corrected with minor changes. These changes do not impact the academic content of the article.

Article highlights

- Hazard analysis of GLOF was estimated using the AHP method.
- Identification of critical lakes with respect to various basins based on overlay analysis.
- Lake morphodynamics is studied on a sub-basin scale in the whole Himalaya.

the 1990s and 2000s, glaciological studies primarily relied on medium-resolution optical satellite data such as Landsat and ASTER, which, despite its utility, was limited by relatively coarse spatial resolution (30 m) and restricted temporal coverage (e.g. Redpath et al. 2013; Mohanty and Maiti 2024). However, the launch of Sentinel-2 by the European Space Agency (ESA) offered free and open-access optical data with up to 10 m spatial resolution, which has considerably enhanced the capacity for detailed and frequent monitoring of glacial environments (e.g. Wangchuk and Bolch 2020). Additionally, the Indian Remote Sensing (IRS) LISS-IV sensor provides high spatial resolution optical data at 5 m, further supporting fine-scale analysis. Furthermore, the accessibility of high-resolution digital elevation models (DEMs) has notably improved. Commercial satellite missions such as WorldView-3 and WorldView-4, GeoEye, Pléiades, and IKONOS provide very high-resolution stereo imagery capable of generating DEMs with spatial resolutions ranging from sub-metre to 1 m (Huggel and Kääb 2006; Armstrong et al. 2016). These datasets are indispensable for accurately mapping glacier surface topography, estimating volume change, identifying past GLOFs, and modelling potential flood inundation areas in the event of GLOFs. Collectively, the integration of freely available medium-to-high-resolution optical data, along with commercially available very high-resolution imagery and DEMs, has opened new avenues for precise, multi-temporal, and multi-sensor-based glaciological research and hazard assessment in cryospheric regions (Shugar 2021; Sattar 2025).

Among the various existing GLOF databases, the most recent and comprehensive inventory was compiled by Lützow et al. (2023), encompassing the entire globe. The second most recent inventory was developed by Shrestha (2023) specifically for High Mountain Asia. A total of 3151 GLOFs were recorded globally between 850 and 2022 CE (Lützow et al. 2023). Among all the glaciated parts of the world, the Himalayas has the third-highest number of GLOF occurrences after North America and Iceland (Carrivick and Tweed 2016; Lützow et al. 2023). In the Himalayas alone, Lützow et al. (2023) have listed 422 GLOF events since 850 CE, while Shrestha et al. (2023) have documented 703 GLOF events since 1533. Table 1 summarises the downstream impact of all the Himalayan GLOFs. Analysis of these GLOF databases revealed two regional peak distributions of previous GLOFs in the Himalayas: one near the western Himalayas and the other in the Everest, Bhutan, and Sikkim regions (Eastern Himalaya) (Figure 1). Among all mountainous regions, the Hindu-Kush-Himalayas (HKH) has the highest exposure to GLOF hazard as the seismic activity (i.e. due to the region's structural geomorphology) makes it vulnerable to extreme events such as slope failure, snow/ice avalanches, and rockfalls that ultimately trigger GLOF (e.g. Banerjee 2025). More than half of the global exposed population is found in just four countries: India, Pakistan, China, and Peru (Andes) (Taylor et al. 2023). Consequently, the Himalayas demand urgent attention, and effective mitigation measures must be implemented to address the escalating risk of GLOF events. Proactive steps are crucial to mitigate potential damage and protect local communities and infrastructure from future hazards.

From the GLOF inventory datasets, it is clear that the GLOF occurrence has been increasing in the Himalayas from 1533 to 1990, after which this trend flattened (Carrivick and Tweed 2016; Harrison 2018; Nie et al. 2020). Previous studies show that GLOF occurrences will increase in the 21 st century in the lower Indus, Ganges and Brahmaputra rivers (e.g. Hirabayashi 2013; Wijngaard 2017). The GLOF frequency is seen to have increased after 2023 with three GLOF events including the South Lhonak lake GLOF (Zhang et al. 2024) in the Sikkim Himalaya, Birendra Lake GLOF in the Gorkha district of Nepal (Khadka et al. 2024), and the GLOF in the Everest region in Nepal (https://www.icimod.org/press-release/glof-from-thyanbo-glacial-lake-sweeps-away-thame-village), occurring in 2024 alone.

Most of the GLOFs have created havoc on the community, livestock, agricultural land, as well as infrastructure downstream in the Himalayas (Nie et al. 2020; Mondal 2025). This highlights the urgent need to assess risks from various triggering mechanisms, particularly in the Himalayas, where 68% of hydropower plants are situated along potential GLOF pathways (Schwanghart et al. 2016). For example, the Luggey Tso flood totally

Table 1. Documented Glacial Lake Outburst Flood (GLOF) events in the Himalayas since 1950, detailing the triggering causes, type of glacial lake, source lake name, and corresponding downstream impacts.

Year	Lake name	Glacier name	Lat	Lon	Lake type	Country	River basin	Driver GLOF	Impact
1560	Unknown	Machhapuchhre	28.52	83.992	Supraglacial	Nepal	Seti	Unknown	50–60 m thick debris covering Pokhara basin
1879	Unknown	Chong Kumden	35.172	77.702	Ice dammed	India	Shyok	Surging glacier	estimated discharge from observed rise at Attock
1882	Unknown	Chong Kumden	35.172	77.702	Ice dammed	India	Shyok	Surging glacier	estimated discharge from observed rise at Attock
1954	Sangwang Co	Unnamed	28.2388	90.109	Moraine dammed	China	Nian Chu	Ice calving	Damaged Shigatse city and villages along the Yarlung Zangbo river, 200 kms away from the lake with a peak discharge 10 k m^3s^{-1},
1957	Tarina Tsho	Unnamed	28.104	89.899	Moraine dammed	Bhutan	Pho Chhu	Ice avalanche	The Punakha Dzong building, 75 km downstream from the lake was damaged
1959	Tarina Tsho	Unnamed	28.104	89.899	Moraine dammed	Bhutan	Pho Chhu	Unknown	The Punakha Dzong building, 75 km downstream from the lake was damaged
1964	Gelhaip Co	Unnamed	27.964	87.816	Moraine dammed	China	Pumqu	Ice avalanche	Damaged Chentang-Riwo Highway
1964	Damenhai Co	Unnamed	29.86768	93.04072	Moraine dammed	China	Gongbujiangda/ Tangbulang (Nyang)	Ice avalanche	Blocked the Niyang River for 16 h
1980	Nagma Pokhari (Phuchan)	Unnamed	27.869	87.867	Moraine dammed	Nepal	Tamor	Moraine collapse	Destroyed villages 71 km downstream from the source
1981	Cirenma Co	Zhangzangbo	28.067	86.065	Moraine dammed	China	Poiqu	Ice avalanche	dammed Poiqu River destroying Quxiang Village
1985	Dig Tsho	Langmoche	27.874	86.594	Moraine dammed	Nepal	Dudh Koshi	Ice avalanche	60 km
1994	Luggye Tsho	Unnamed	28.092	90.299	Moraine dammed	Bhutan	Pho Chhu	Landslide	damaged Punakha Dzong
1997	Kongyangmi La Tsho	Unnamed	27.9	88.78	Moraine dammed	India	Changme	Ice avalanche	7.5 km from the source
2001	Chongbaxia Co/ Longjiu Co	Unnamed	28.21111	89.74499	Moraine dammed	China	Nian Chu	Unknown	15 km from the source
2013	Chorabari	Chorabari	30.747	79.064	Moraine dammed	India	Alaknanda	Intense rainfall	300 m
2015	Lemthang Tsho	Unnamed	28.069	89.58	Supraglacial	Bhutan	Mo Chhu	Intense rainfall	30 km from the source
2017	Langmale	Barun	27.814	87.141	Moraine dammed	Nepal	Arun	Rockfall	downstream riverside communities in Bhojpur and Dhankuta, displaced 10 families
NA	Unknown	Glaciers in Lunana	28.0351	90.3099	Unknown	Bhutan	Pho Chhu	Unknown	destroyed Punakha dzong
2023	South Lhonak Lake	South Lhonak glacier	27.947	88.331	Moraine dammed	India	Tista	Lateral Moraine failure	>300 km impact downstream, 1 hydropower plant destroyed 14 bridges got washed away and many kms of roads destroyed 47 people lost their life.
2024	Birendra lake	Manaslu Glacier	28.596	84.629	Moraine dammed	Nepal	Gandaki river	Ice avalanches	Downstream minor impact, destroyed the makeshift bridge near Chumanuwri Rural Municipality
2024	Thyanbo glacial lake	Thyanbo glacier	27.821	86.571	Moraine dam lake	Nepal	Dudh Kosi	Ice Avalanches	14–20 structures including a school, hotel, and health post were destroyed, while 135 residential buildings were damaged.

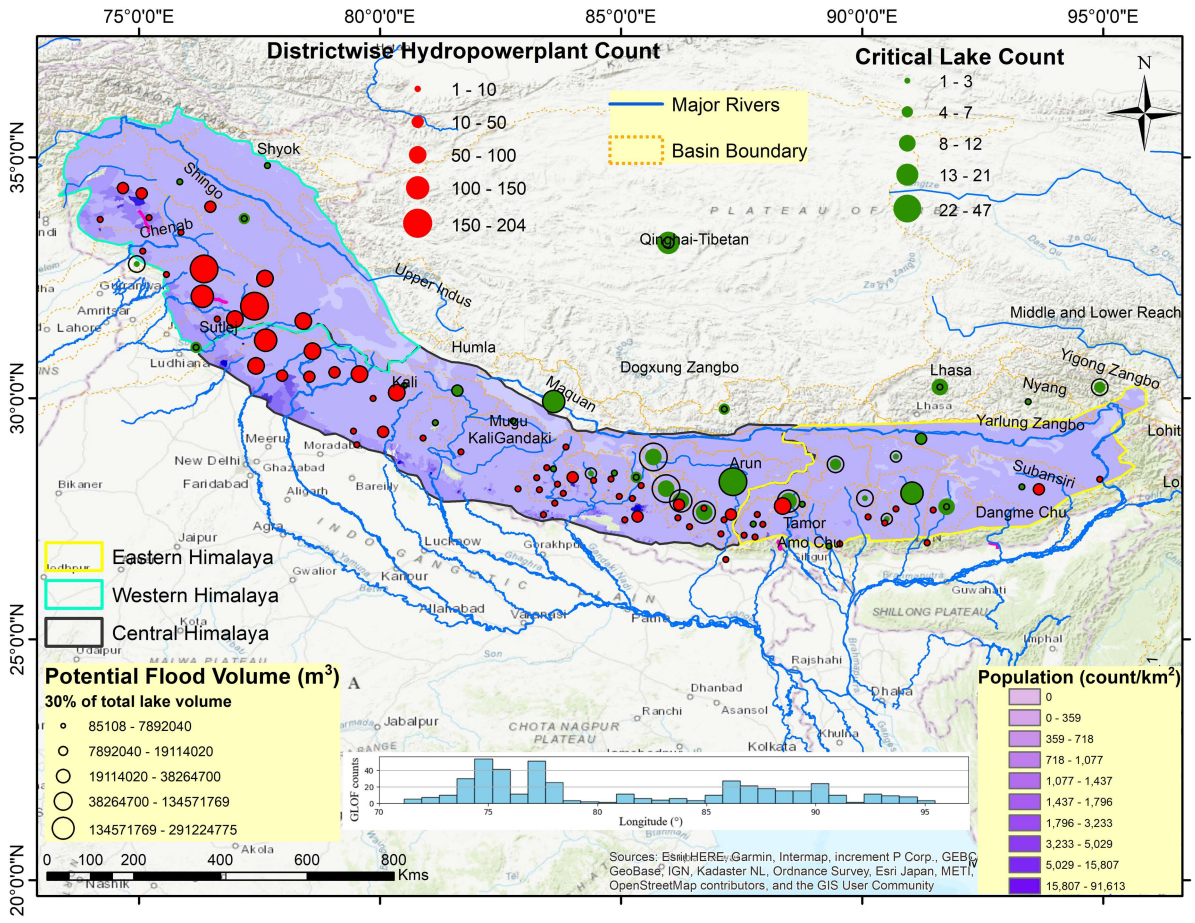

Figure 1. Himalayas is shown here as a study area that is classified as eastern, central and western, shown in yellow, green and cyan colour, respectively. Critical lake count and potential flood volume distributions are shown in the green circles and hollow circles, respectively, for different sub-basins of the Himalayan region. The hydropower plant count is shown district-wise in red circles along the Himalaya. Population density is shown in the Himalayas in a violet colour grading scale. The past GLOF events are shown in a frequency graph below.

damaged a hydropower plant estimated to be ~$500 million in 1994 (Shrestha et al. 2010). Recently, the South Lhonak GLOF destroyed the Chungthang hydropower project, which cost around $US 16 billion (Yu et al. 2024). The Chamoli flash flood swept away the unfinished Tapovan Vishnugad hydropower project and inflicted substantial damage on the Rishi Ganga hydropower project (Shugar 2021; Mondal and Bharti 2022). The Dig Tsho GLOF in 1985 destroyed the NAmche Hydro-power plant that was valued at $US 3 million and also completely destroyed about 30 houses, and 14 bridges between Mingbo and Jubing (Bajracharya 2009). In 1981, a GLOF event in Nepal damaged Friendship bridge of Nepal-China Highway and Koshi power station with heavy economic losses (Bajracharya 2009; Sattar et al., 2022). A GLOF (Cirenmaco Lake/Zhangzangbo Lake) event that occurred during August 2000 damaged 98 bridges in the Tibetan Plateau and destroyed around 10,000 houses, accounting for about $US 75 million of financial loss (Nie et al. 2018). Thus, measures should be taken to minimise the devastating nature of GLOF towards costly infrastructure.

Documentation of critical glacial lakes, downstream impact analysis and application of remedial measures can prevent various upcoming calamitous GLOFs. Therefore, in this paper, we will be discussing four aspects of glacial lakes, i.e. the latest lake distribution in the Himalayas, ii. Lakes change and their dynamics, iii. critical lake distribution in the Himalayas, and iv. Hazard zonation in the Himalayas. To our knowledge, this is the first pan-Himalayas hazard assessment of the critical glacial lake basins. We aim to answer the following science questions:

1. Which glacial lake basins' hazard levels are at maximum and minimum?
2. Which parameter (i.e. among population density, potential flood volume, critical lake count, and infrastructure) has the maximum impact on deciding the hazard levels of the lake basins?

2. Study area

Himalayas consists of rugged topography ranging from 1000 to 8848 m in elevation above the mean sea level, and encompasses the highest elevation of the Earth, named Everest, with an elevation of 8848 m (Figure 1) (Mohanty and Maiti 2024). The Himalayas is a 2500 km-long orogenic zone that varies in width from 400 km in the west to 150 km in the east (Rubatto et al. 2013). The Himalayas is a major part of High Mountain Asia, which is bounded by 69° 48′ 36.73″ E longitude to 98° 22′ 22.78″ E and 27° 12′ 16.89″ *N* to 39° 31′ 26.89″ *N* latitude. The Himalayas is classified into three major parts based on geographic and topographic patterns, namely eastern, central, and western Himalayas (Bolch 2012). The glacial lakes in the Himalayas are distributed in the three major river basins: Indus (362), Brahmaputra (722), and Ganga (354) (Shugar 2020). Moreover, GLOF, landslide lake outburst flood (LLOF), landslides, avalanches, and earthquakes are major concerns for developing countries located near the periphery of these mountain chains.

The distribution of glaciers and equilibrium line altitudes are mainly due to three types of wind flows, such as (i) northwest wind flow (westerly), (ii) southwest Indian monsoon, and (iii) northeast wind flow (Bookhagen and Burbank 2006; Bolch 2012). The Eastern Himalayas gets snow from the SW Indian monsoon and the NE wind flow, mainly during the summer, thus it is called the summer accumulation zone. This zone contains the glaciers, which are called the summer accumulation type. The western side of the Himalayas (i.e. Karakoram, Pamir, and western Himalaya) gets the snow from westerly winds during the wintertime; hence, it is called the winter accumulation zone, and the glaciers are of the winter accumulation type. Indian monsoonal precipitation decreases from east to west, and the western extremity of the monsoonal precipitation zone is present at 78° longitudes near Sutlej valley (Bookhagen and Burbank 2006). The northern side of eastern Himalayas gets fewer snowfalls than the southern side by monsoonal precipitation due to the shadow effect (Bookhagen and Burbank 2006). Besides, the northern part of the Himalayas and the southern part of the Tibetan plateau get precipitation from the NE wind flow during the winter time, sourced from the Siberian region.

3. Data and methods

3.1. Glacial lake, GLOF and critical lake inventory

Glacial lake inventory datasets of Zhang et al. (2015), Wang et al. (2020), Shugar (2020), Mohanty et al. (2023a), and Zhang (2023) were utilised in this study. The details of the each of these used glacial lake inventory data mentioning year of study, size of lake, count of lake are presented in Table 2. We used the extensive inventories of glacial lakes available for the Himalaya. Besides, GLOF inventory of Lützow et al. (2023) and Shrestha (2023) for the Himalayas only were utilised in this study. The inventory of critical (or Vulnerable) lakes was accessed from six different sources i.e. Wang (2013), Shijin et al. (2015), Dubey and Goyal, (2020), Wang et al. (2020), Mohanty and Maiti (2021b), and ICIMOD (Bajrachary et al. 2020). We conducted an overlay analysis of critical lake datasets from multiple published studies to identify distinct and unique critical glacial lakes distributed across the Himalayan region. The majority of critical lakes considered in this study are moraine-dammed and ice-dammed lakes that have maintained a consistent spatial position over time.

Various researchers have identified critical lakes in the Himalayas using a range of data integration methods and parameters (Washakh et al. 2019; Maurer 2020; Mohanty and Maiti 2021b). The methods include: estimating the rate of change of glacial lake-area (based on satellite imagery), estimating the risk of landslides or avalanches triggering a GLOF, calculating lake volume by measuring lake bathymetry or via

Table 2. Lake size and number distribution in different years by different researchers.

	Lake size (km^2)						Lake number					
	1990	2000	2005	2010	2015	2018/2020	1990	2000	2005	2010	2015	2018/2020
Zhang et al. (2015)	253.38	272.95	*	329.77	*	*	2089	2251	2585	*	*	*
Wang et al. (2020)	525.19	*	*	*	*	615.94	7111	*	*	*	*	8070
Shugar (2020)	*	139.17	217.02	225.73	223.69	224.95	*	588	876	888	861	950
Mohanty et al. (2023b)	664.75	660.22	*	800.3	492.01	2075.35	5194	5222	*	6432	6481	8357
Zhang (2023)	666.41	676.61		724.17	749.61	779.01	7334	7361		7833	8143	9208

empirical relationship between lake area and lake volume, inspecting the stability of the lake's moraine dam by exploring the presence of dead ice through field observation, identifying calving prone lakes based on satellite imagery, calculating probable flood volume and intensity (Wang 2013; Aggarwal et al. 2017; Mohanty and Maiti 2021b). Other methods include GIS-statistical analysis, overlay analysis, matrix and fusion of vulnerability-cum exposure indices, which have been used by many researchers to identify the critical lakes (Huggel 2004; Kääb and Reichmuth 2005; McKillop and Clague 2007; Allen et al. 2016).

3.2. Population density data

Rasterised data of population density (Gridded Population of the World (GPW), v4) were taken from the Socioeconomic Data and Application Centre (SEDAC) (https://sedac.ciesin.columbia.edu/data/collection/gpw-v3). This dataset represents the population census data collected during the 2011 national population enumeration in India.

3.3. Building, road and railway infrastructure

Existing buildings, railways, and roadways data were obtained from the OpenStreetMap for the Himalayas and their surrounding mountain ranges. The buildings are represented as point features in the OpenStreetMap dataset. From these points, the building point density map was generated for every 6 by 6 kernel. Roads and railway networks were available in vector formats as line features. To obtain the density of roads and railways, a line density tool was utilised in a GIS platform. These are the updated data specifically for the year 2020.

3.4. Hydropower plant data

The data for existing and future planned hydropower projects were downloaded from the published results of Zhang (2023) (http://globaldamwatch.org/grand/). To augment this dataset, we also conducted a comprehensive manual review of various documents and reliable online sources to gather information on the existing and planned hydropower plants located in the Indian, Nepalese, and Bhutanese-administered regions of the Himalayas. In total, we identified 1242 hydropower plants that have been established or are planned to be established over the next 15 years in the entire Himalayas. Thus, these are the updated data for hydropower plants for the year 2024. For every basin, we also estimated the density of the hydropower plants using a 6-by-6 kernel in a GIS platform. Here, we used a 6 by 6 kernel size for the density estimation to match the previously derived road, railway, and lake densities.

3.5. Estimation of probable GLOF volume

We considered only ice-dammed and moraine-dammed lakes for this glacial lake hazard assessment in the Himalayas. Basin-wide estimation of lake volume was done using the volume–area scaling method (e.g. Cook and Quincey 2015; Banerjee 2024).

$$V = 0.1217 * A^{1.4129} \quad (1)$$

Here, V and A are the lake volume and lake area in km^3 and km^2, respectively.

In addition to the aforementioned parameters, it was assumed that a minimum of 30% of the total glacial lake volume would be released during a potential GLOF event, following the observations of Lützow et al. (2023) who had compiled the global list of hazard discharges that were released during GLOFs. Among the list of reported values, 30% was the lowest discharge volume that was reported. Therefore, we made this choice to delineate the lower-bound hazard zonation downstream, thereby highlighting areas that are at risk even under conservative outburst scenarios. Accordingly, a threshold of 30% of the total lake volume was adopted for estimating the minimum potential flood volume in this study.

3.6. Estimation of GLOF hazard

The risk from any disaster event is represented as a function of hazard, exposure, and vulnerability, while hazard is a function of intensity and probability of occurrences (IPCC 2014). In this study, we are estimating the extensive hazard by incorporating exposure, hazard intensity, and probability. However, since our analysis does not account for key socio-demographic and socio-economic variables such as age distribution, sex ratio, literacy rate, household income, employment status, access to healthcare and education, infrastructure availability, land ownership, economic dependence, and housing quality, it cannot be classified as a comprehensive vulnerability assessment. Consequently, without integrating these factors, we do not proceed to quantify risk in this work.

Here, we integrate these three major components in the analytical hierarchy process (AHP). The analytical hierarchy process (AHP) was employed in this study, as it is a well-established and suitable multi-criteria decision-making tool for estimating extensive hazard potential at a basin scale, which aligns with the primary objective of this paper. AHP facilitates the assignment of relative weights to multiple contributing parameters based on expert judgement in a transparent and structured manner, offering a distinct advantage over other available techniques. Furthermore, as the focus of this research is limited to assessing extensive hazard potential in the Himalayan region – without extending into risk or vulnerability estimation – we did not adopt methods such as the hazard-vulnerability matrix or similar integrative risk assessment frameworks, which typically require detailed vulnerability and exposure analysis beyond the scope of this study. However, hydrodynamic modelling of outburst floods for intensity mapping was not conducted, which remains a crucial component for accurate exposure estimation. Instead, critical lake (vulnerable) density and estimated probable flood volume were employed as proxy indicators to represent intensity in the mapping process. Given the high critical lake counts in the expansive Himalaya, it is not feasible to create an intensity map for every single lake. Besides, exposure is the component directly connected to the presence of people, livestock, agricultural land, environmental services, and other costly infrastructure along the floodplain (Allen et al. 2019). In this component, we included hydropower plants, railways, roads, and buildings. Additionally, vulnerability is a component that is directly proportional to how living beings are affected by hazards. In our assessment, we included population count as a key factor for estimating exposure. However, livestock data could not be included in this analysis due to the extensive size of the study area, which made it challenging to gather accurate and comprehensive information on livestock distribution.

In this paper, we combine all the parameters, namely probable flood volume, critical lake density, building density, road and railway density, and population density, for assessing the hazard in the Himalayas. Finally, probability, intensity, and exposure were combined using a data integration method (AHP and GIS) to produce the hazard level of each basin-wise (Figure 2). Instead of using simple matrix methods to combine hazard, exposure, and vulnerability, we assigned weightings to each parameter to generate the final raster map displaying risk levels. We reclassified all input parameters into quartile classifications, resulting in six classes, and AHP-derived weights were assigned to each layer for integration into the hazard assessment. We used the AHP calculator to estimate weightage (Uyan 2013; Mohanty and Maiti 2021b). Population density was given the highest weight, followed by critical lake counts, hydropower plants, potential flood volume, and building and road construction.

In the AHP, the consistency ratio (CR) measures how consistent the pairwise comparisons are in the decision matrix i.e. how logically coherent a decision maker's judgements are. The CR ratio is defined as:

$$\mathrm{CR} = \mathrm{CI}/\mathrm{RI} \tag{2}$$

where the CI (consistency index) and RI (random index) are defined as follows:

$$CI = \frac{\lambda_{\max} - n}{n - 1} \tag{3}$$

where λ_{max} is the maximum Eigen value, which in turn is estimated as:

$$Aw = \lambda_{\max} w \tag{4}$$

Priorities **a**

These are the resulting weights for the criteria based on your pairwise comparisons:

Cat		Priority	Rank	(+)	(-)
1	Critical lake count	25.6%	2	18.4%	18.4%
2	Potential flood volume	14.2%	4	5.3%	5.3%
3	Population	29.6%	1	11.0%	11.0%
4	Building	8.7%	5	3.5%	3.5%
5	Roads	4.9%	6	1.9%	1.9%
6	Hydropower	16.9%	3	10.2%	10.2%

Number of comparisons = 15
Consistency Ratio CR = 9.7%

Decision Matrix **b**

The resulting weights are based on the principal eigenvector of the decision matrix:

	1	2	3	4	5	6
1	1	1.00	1.00	2.00	3.00	4.00
2	1.00	1	0.33	2.00	2.00	1.00
3	1.00	3.00	1	2.00	6.00	3.00
4	0.50	0.50	0.50	1	2.00	0.25
5	0.33	0.50	0.17	0.50	1	0.17
6	0.25	1.00	0.33	4.00	6.00	1

Principal eigen value = 6.611
Eigenvector solution: 7 iterations, delta = 5.5E-9

Figure 2. Weightage values derived for each parameter from the AHP calculator are listed in (a), while in (b) the decision matrix from the pairwise comparision is shown; the consistency ratio and decision matrix are also shown here for hazard estimation.

Here, A is the pairwise comparison matrix whose entries (i.e. a_{ij}) represent the importance of parameter i with respect to j, and w is the priority vector or Eigen vector. This is computed by first a) normalising each column of A, followed by b) averaging each row of the normalised columns. For consistent judgements, the value of CR must be less than 10%. In our analyses, the value of the CR was estimated to be ~9.7%, indicating consistency.

For flood intensity estimation, we considered a threshold of 30% of the total probable flood volume. In hazard analysis, we combine all these parameters, i.e. exposure and hazard, by assigning weights derived from the AHP calculator to each of these parameters (population density, critical lake density, probable flood volume, hydropower plant density, road density, railway density, and building density) (Figure 3).

4. Results and discussion

4.1. Glacial lake distribution and dynamics in the Himalaya

We analysed the spatial distribution of glacial lakes across the Himalayas using five published datasets, namely Zhang et al. (2015), Wang et al. (2020), Shugar (2020), Zhang (2023), and Mohanty et al. (2023a) (Figure 4). For a comprehensive and statistical assessment of lake area change rates and their distribution at the basin scale, we employed the dataset from Zhang (2023), as it represents the most extensive, detailed, and up-to-date compilation available among the five datasets considered. These lakes are prominent in the region with the highest degree of glacial retreat, and the retreat depends on glacial, topographic, and climatic factors (Bolch 2012; Bhambri 2023; Pandey 2024). From the histogram plot (Figure 4), we noticed that most of these glacial lakes are present in Langtang, Bhutan, Sikkim, and the Everest region, i.e. between the longitudes 83° E and 94° E, respectively. A total of 24,440 glacial lakes were detected in the Himalayas, out of which 12,100 are the supra-glacial lakes, while the rest include the lakes that are proglacial, erosional, rock dams, valley blocked, etc. Moreover, most of these lakes are located at an elevation between 4500 and 5500 m (Figure 5). A total of 10,101 lakes with a size greater than 0.01 km^2 are noted in the Himalayas, as extracted from the utilised inventories. A continual increase in frontal loss of glaciers has led to the creation of new space for lake area expansion to higher elevations, as shown in Figure 5. Additionally, pristine lakes are continuously forming at a higher elevation (Figure 5). Glacial lake count and total area have been continuously increasing in the Himalayas year-wise (Table 2).

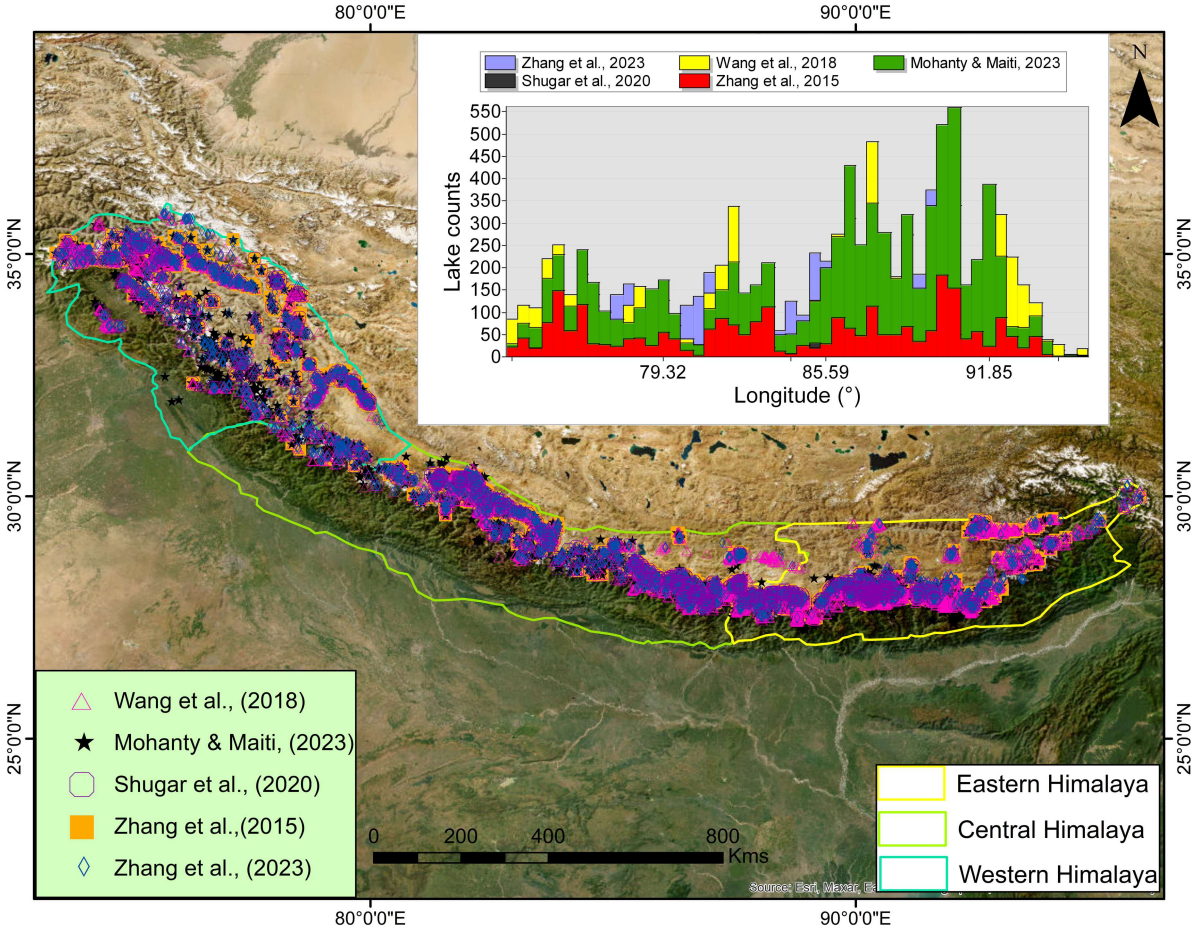

Figure 3. The latest glacial lake's distribution is shown for Himalayas which is extracted from different previously performed studies: black star (Mohanty and Maiti 2021b), hollow diamond (Zhang 2023), red hollow circle (Shugar 2020), green hollow triangle (Wang et al. 2020), brown square (Zhang et al. 2015).

4.2. Distribution of lake area, number, and their dynamics

We summarised the lake count, total, and average lake area distribution in different sub-basins of the Himalayas (Figure 6). The lake count is maximum in the Kosi basin (sub-basin Arun = 1125), followed by Yarlung Zangbo (773), Manas (sub-basin Dangme Chu = 715), and Upper Indus (619). In terms of total lake area distribution, the largest contributions come from the Qinghai-Tibetan, Yarlung Zangbo, Panjnad, Kosi, Manas, and Upper Indus basins. Meanwhile, the basins with the highest average lake area include those from the Qinghai-Tibetan, the Yarlung Zangbo, the Panjnad, the Phelku, the Upper Indus, and the Koshi regions (Figure 6). Based on the overlay analysis of total lake count, total lake area, and average lake area, we found four critical basins, namely Kosi, Yarlung-Zangbo, Manas, and Upper Indus.

Additionally, in the Himalaya, the lake-area growth was identified as 30%, 17%, 76%, 20% and 26% from the dataset of Zhang et al. (2015), Wang et al. (2020), Shugar (2020), Zhang (2023) and Mohanty et al. (2023a), respectively, in different time periods (mostly between 1990 and 2020). Additionally, the highest lake-area growth was identified between 2010 and 2020 in all data sets, while the lowest was for the period 1990–2000. These decadal growth rates (i.e. 1990–2000 and 2010–2020) showed that the area of the glacial lakes is increasing with time. This increase in lake area corresponds with the rise in glacial retreat. Lake-area growth is highest in the elevation band of 4000–5000 m (Mohanty et al. 2023b). Lake area growth was found to be higher for a connecting moraine dam lake than for an unconnected lake and a non-glacier-fed lake (Wang 2013; Song et al., 2014; Song et al., 2017; Zhang et al. 2015; Mohanty and Maiti 2021b).

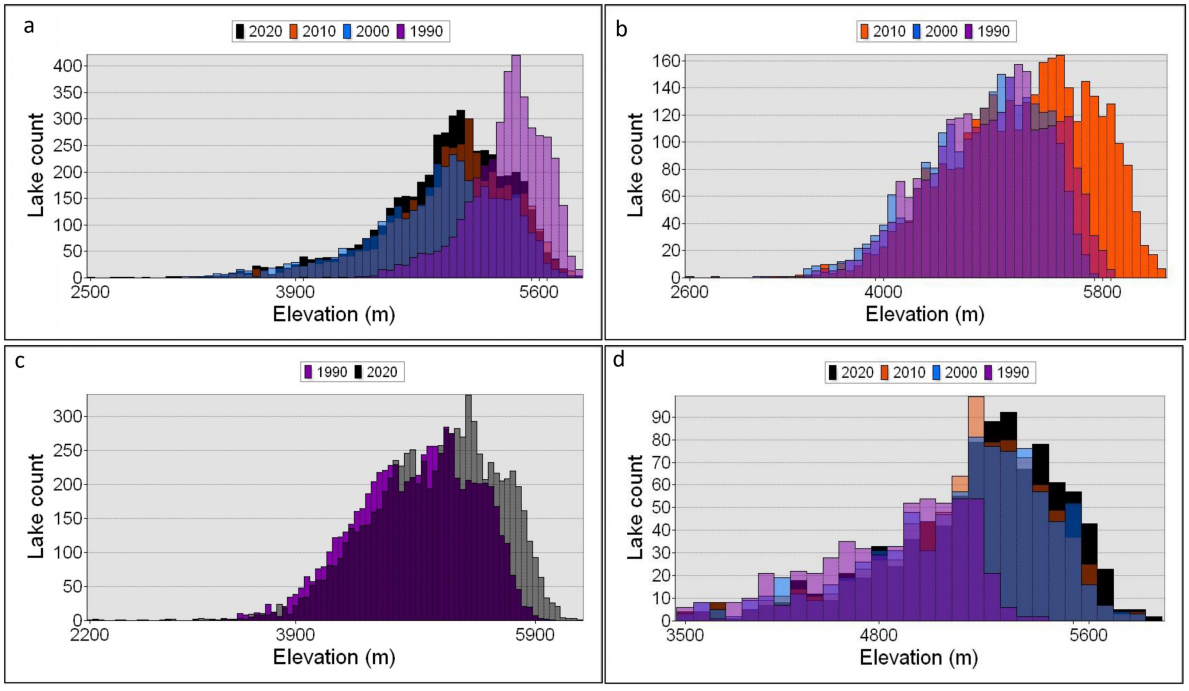

Figure 4. Glacial lakes' distribution with respect to elevation is shown, taken from different previous studies: a. Mohanty et al. (2023b), b. Shugar (2020), c. Wang et al. (2020), d. Zhang et al. (2015). Here, various colours show the lake distribution with respect to elevation in different years.

The basin-wise average lake area change rate is found to be highest in the Upper Indus, Karnali, Tista, Yamuna, and Manas basins. The highest glacial lake area change rates were observed in the Kosi, Yarlung Zangbo, Manas, Karnali, Upper Indus, and Tista basins, suggesting that these regions are the most susceptible to potential future GLOF events (Figure 7). Additionally, basins exhibiting the lowest minimum glacial lake size change rates are primarily located in the Kosi (Tama Pokhari, Tsho Rolpa GLOF), Tista (South Lhonak lake), Upper Indus (Suru lake GLOF), Manas (Lugge Tsho), and Yarlung Zangbo (Chongbaxia Tsho GLOF) basins, indicating a higher likelihood of having experienced GLOF events in the past. This hypothesis was further validated using existing GLOF inventory data, which revealed a strong correspondence between areas with lower minimum lake size change rates and documented historical GLOF occurrences. From the GLOF inventory, we also identified these basins, which have a very high number of GLOF events: Hunza (23), Yarkant (13), Chitral (8), Gilgit (7), Humla (6), Dudh Kosi (5), and Poique (3).

4.3. Critical lake distribution in the Himalaya

Here, six different datasets were used, showing critical lakes with varying spatial distributions in the Himalayas (Figure 8). Overlay analysis was performed to identify the spatial distribution of critical glacial lakes in the Himalaya. A total of 221 critical lakes were identified in the Himalaya, and these critical lakes are mostly located in the eastern and central parts of the Himalaya. Sub-regionally, Everest (38), Sikkim (34), Bhutan (17) and Langtang (14) regions contain very high numbers of critical lakes, while the western Himalayas have comparatively less in numbers (Figure 8). Moreover, the Kosi basin contains the highest number of critical lakes (47), followed by Yarlung Zangbo (22), Tista (22), Manas (21), Qinghai-Tibetan (15), Panchnad (12), and Phelku (8). Thus, living beings and costly infrastructures closer to Everest, Langtang, Bhutan, and Sikkim are at the highest risk of GLOF. However, the exact impact zone and risk will be estimated after using hydrodynamics modelling in various critical basins.

4.4. GLOF hazard in the Himalaya

Critical lake density is highest in the Kosi River Basin (47), followed by Yarlung Zangbo (22), Tista (22), Manas (21), Qinghai-Tibetan (15), Panchnad (12) and Phelku (8) (Figure 3). Thus, the potential flood

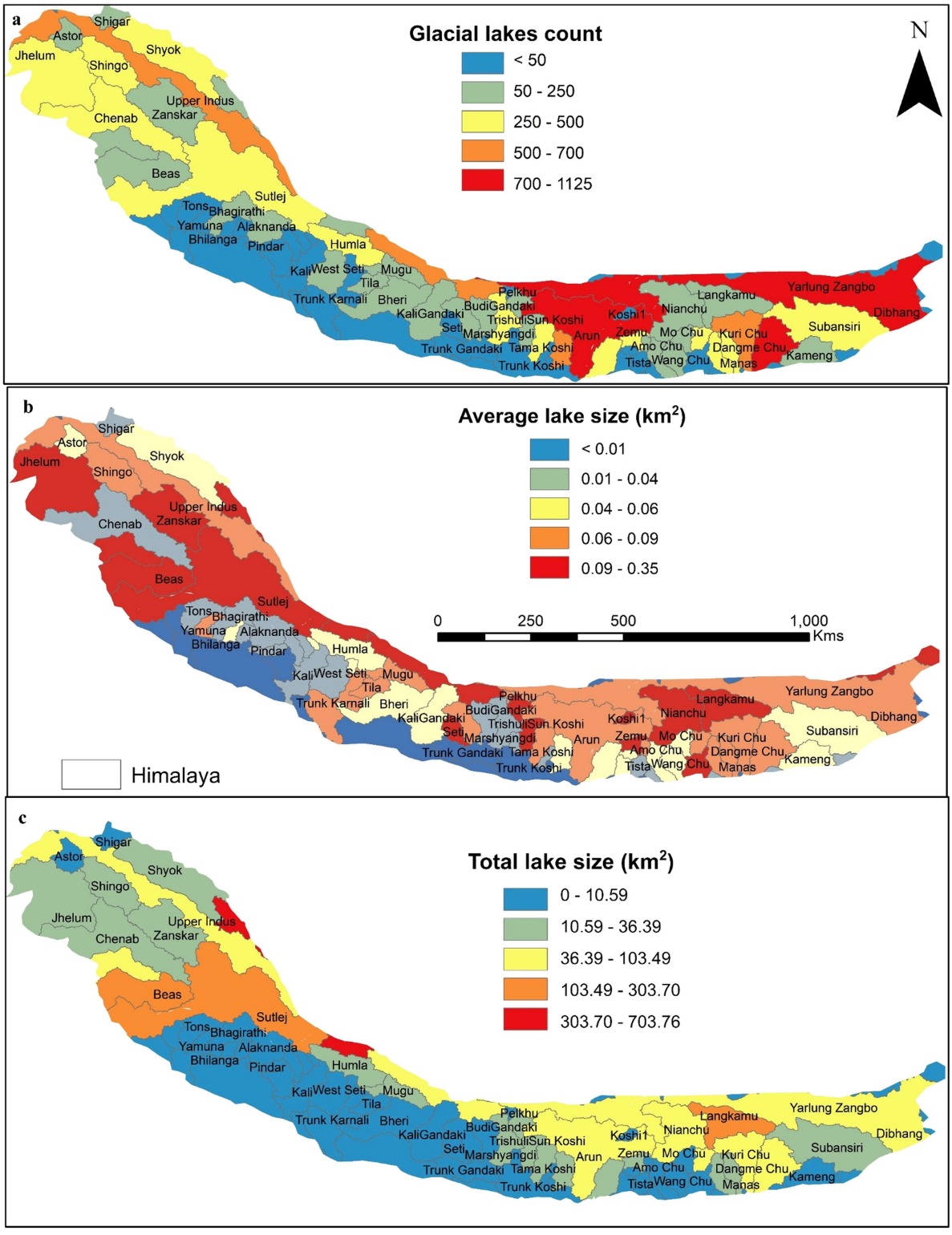

Figure 5. Basin-wise distribution of lake counts (a), average lake size (b) and total lake size (c) is shown in the Himalaya. Here, red, yellow and green colours show the high, medium and low values, respectively.

volume with a 30% threshold is highest in Kosi, followed by Dudh Kosi, Tama Kosi, Chenab Yarlung Zangbo, Manas, and Kuri Chu basin. The density of buildings is estimated to be high near Nepal and Bhutan, while lower in India and China. The same pattern can be seen in the cases of roads and railways. Population density is highest in Nepal, followed by Himachal Pradesh, Uttarakhand, Jammu & Kashmir

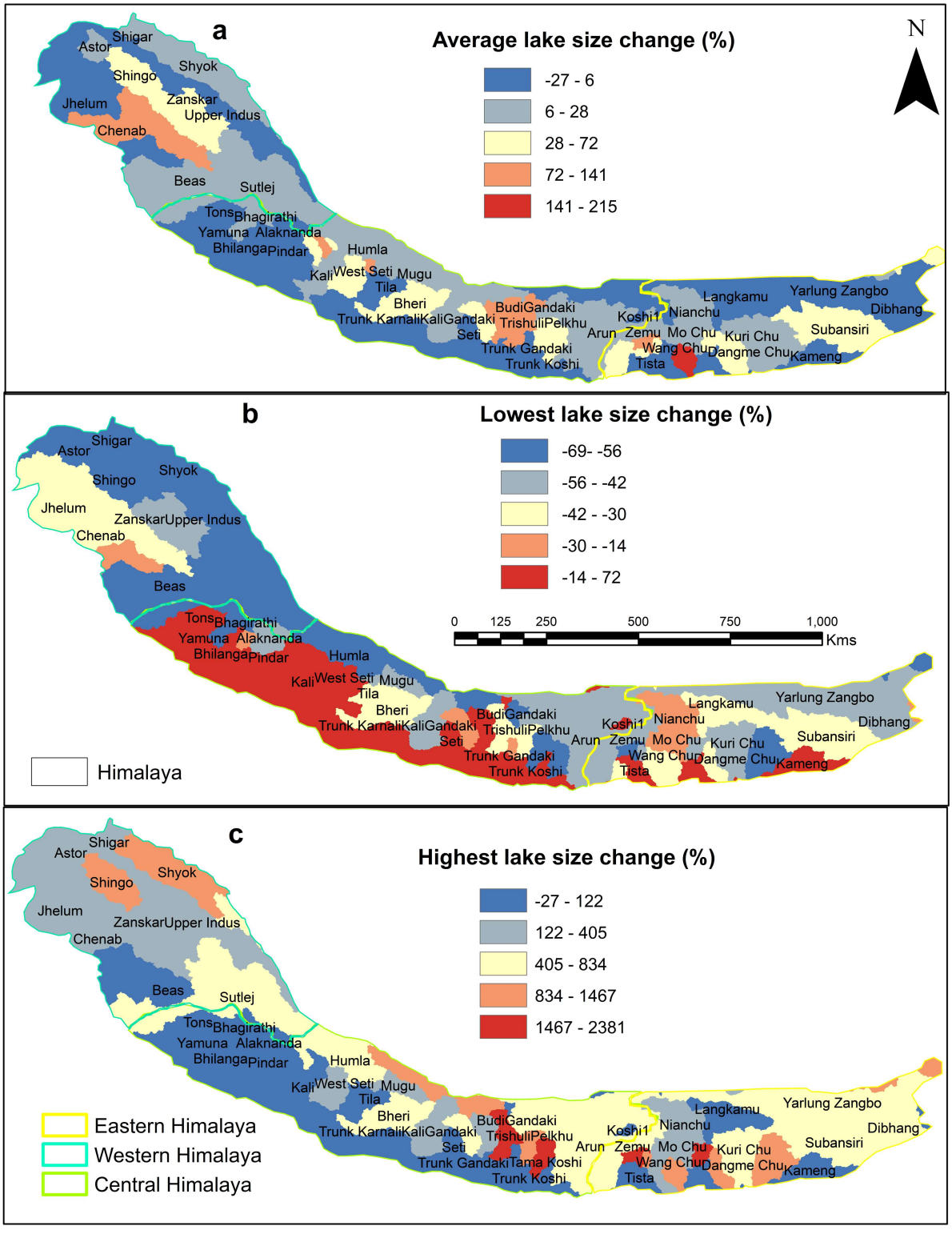

Figure 6. The average (a), minimum (b) and maximum (c) lake size change rate in percentage are shown for various basins in the Himalaya. Here, red, light yellow and blue shade shows the higher, medium and lower values, respectively.

and Bhutan. An extensive distribution catalogue of Hydropower plants was created on the southern slope of the Himalayas, and from the catalogue, it was found that most of the hydropower plants (both operational and those under installation) are located in Himachal Pradesh, followed by Uttarakhand, Nepal, Sikkim, and the Jammu and Kashmir region. The highest number of hydropower plants is

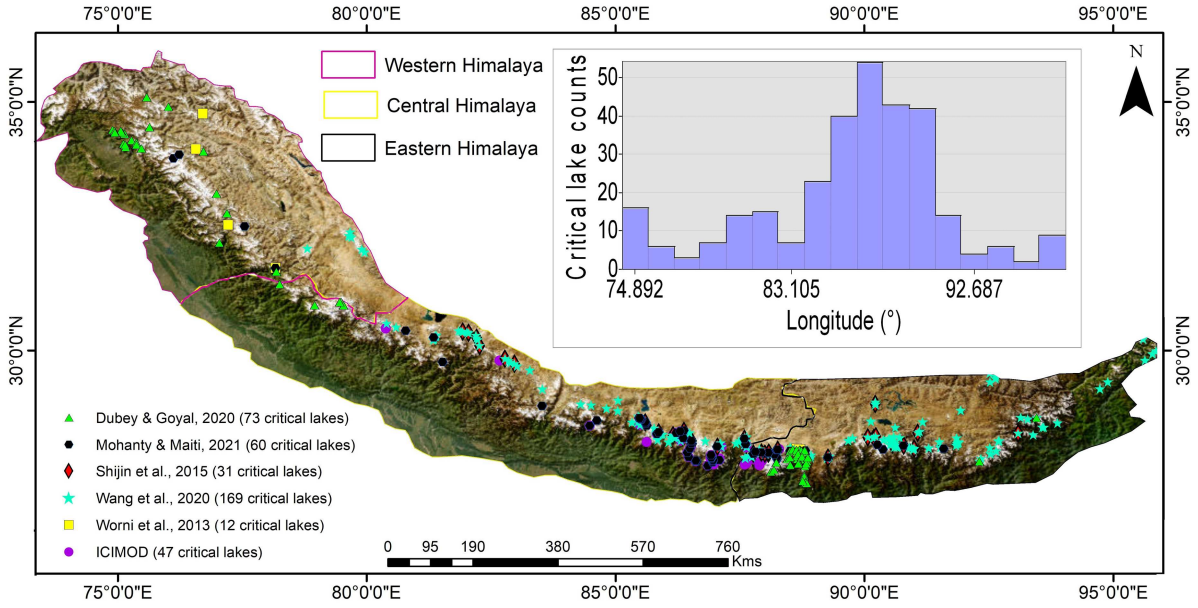

Figure 7. Distribution of GLOF-prone lakes in the Himalayas from different studies: violet circle-Bajracharya et al. (2020) (ICIMOD), green triangle – Dubey and Goyal (2020), blue circle- Mohanty et al. (2023a), yellow square – Wang (2013), red diamond – Shijin et al. (2015), green plus – Wang et al. (2020). Critical lake frequency is shown with respect to latitude and longitude for the Himalayan region in the lower 2 graphs.

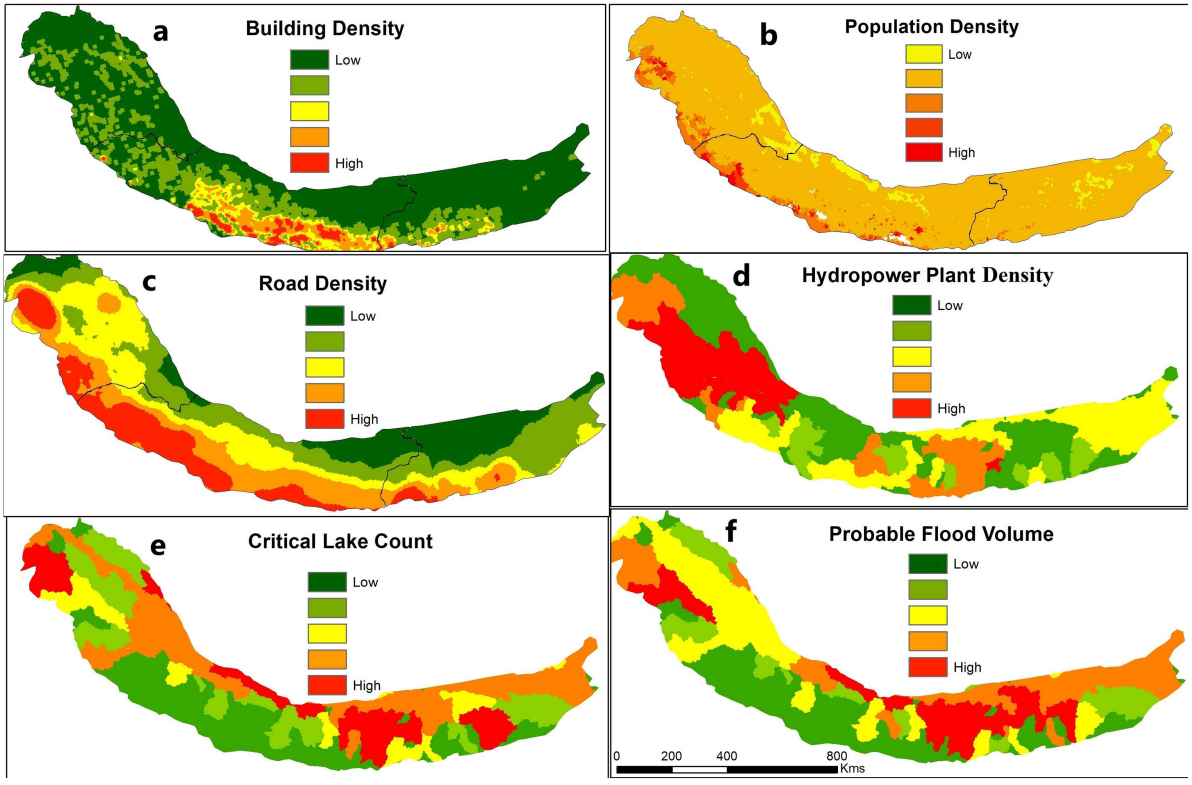

Figure 8. Various layers such as (a) building density, (b) population density, (c) road density, (d) hydropower plant density, (e) critical lake count and (f) probable flood volume in different parts of the Himalayas are shown, and these layers are used for the hazard mapping in the Himalaya. Here, red, yellow and green colours show the represent higher, medium and lower densities, respectively.

distributed across the Beas (384), Ravi (183), Tons (106), Chenab (58), Teesta (55), Kali (40), Sutlej (39), Alaknanda (32), Bhagirathi (31), and Jhelum (28) Basins, in decreasing order.

The Kashmir (Chenab and Jhelum Basin), Himachal Pradesh (Chenab and Beas Basin), Nepal (Koshi, Tama-Kosi, Dudh-Kosi Basin), Bhutan (Kuri chu Basin of the Manas Basin) and Sikkim (Teesta Basin) gave higher hazard score towards outburst flood in the Himalayas (Figure 9). In the Chenab and Jhelum river Basin, the highest number of hydropower plants is located along with the highest road density and probable flood volume. Greater attention should be directed toward these critical basins, particularly due to their high population density and the presence of hydropower infrastructure. Implementing effective management strategies is essential to mitigate the potential intensity of future GLOF hazards.

The areas that were classified to be at very high risk and high risk were found to be located in the Eastern and Central Himalayas (i.e. where the maximum number of GLOFs as well as comparatively larger glacier retreat has been recorded). These regions in the Himalayas are characterised by a greater density of potentially critical glacial lakes and enhanced cryospheric instability, which collectively elevate hazard levels. Many of the lakes located in these regions are connected to glaciers that are heavily debris-covered. Such lakes are often dammed by moraines that are ice-cored, which are susceptible to failure due to continuous subsidence owing to the melting of the ice-core (e.g. the South Lhonak lake GLOF in Eastern Himalayas (Sattar et al. 2025). In addition to moraine dam failure, such lakes are also susceptible to avalanches from the surrounding steep side walls (e.g. Gantayat et al. 2024). In addition, densely populated regions such as Nepal, Sikkim, and Bhutan fall largely within these high-hazard zones, thereby amplifying overall risk through increased exposure. In contrast, the western Himalayas exhibits relatively lower critical

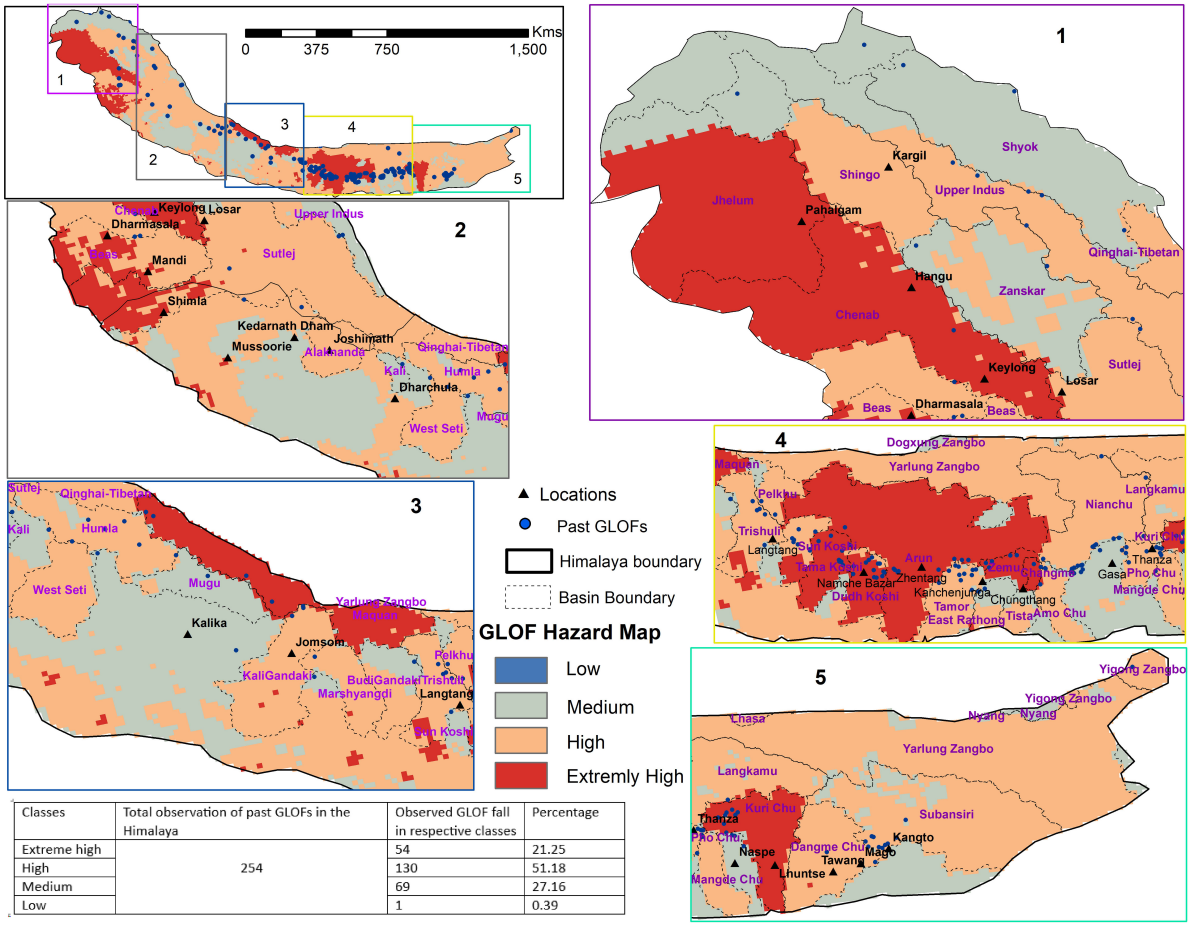

Classes	Total observation of past GLOFs in the Himalaya	Observed GLOF fall in respective classes	Percentage
Extreme high	254	54	21.25
High		130	51.18
Medium		69	27.16
Low		1	0.39

Figure 9. GLOF hazard zonation map of the Himalayan region. Hazard classes are categorised as low (blue), medium (light blue), high (light red), and very high (red). The five inset panels (1–5) highlight representative regions across different parts of the Himalayas to illustrate spatial variability in hazard levels. An accuracy assessment table summarising the model performance is shown in the lower part of the figure.

lake counts and smaller potential flood volumes; however, exposure-related factors, including population and infrastructure density, remain high. Consequently, despite comparatively lower lake-related hazard indicators, basins such as the Chenab and Beas are classified within the higher hazard categories, underscoring the dominant role of exposure in shaping hazard patterns in the western Himalaya.

4.5. Validation of our assessment with respect to observed GLOFs

We compiled a list of 254 events from the latest inventory of GLOFs (i.e. those which occurred in the Himalaya) that was compiled by Shrestha et al. (2023). The inventory spans a time period between 1533 CE and 2024 CE. Among the recorded GLOFs, ~72.4% (184) occurred in the basins that were classified to be at extreme high and high risk, in this study (Figure 9). The lake basins that were classified to be at low risk accounted for 0.39% of the recorded GLOF events. This is a testament to the robustness of our approach.

4.6. Sensitivity analysis and robustness of the AHP framework

A comprehensive sensitivity analysis was conducted to evaluate the robustness of the AHP-derived hazard framework by systematically perturbing the weights of individual parameters while maintaining normalisation and logical consistency. The baseline scenario indicates that population density is the dominant controlling factor, followed by critical lake count, hydropower plant density, and potential flood volume, whereas building and road densities contribute secondary exposure information. In a series of sensitivity experiments, the weight of each parameter was independently increased and decreased by ±20%, and the resulting changes in weights and ranks were examined (see section 1 of Supplementary text). Across all scenarios, the overall rank order of parameters remained largely invariant, with population density consistently retaining the highest rank and critical lake count remaining the second most influential factor. Even under strong perturbations, no parameter exhibited a rank shift exceeding one position, and the Consistency Ratio (CR) remained below 0.1 in all cases, indicating acceptable judgement coherence. These results demonstrate that the hazard assessment is not overly sensitive to individual weighting choices and that the AHP framework yields stable and robust hazard patterns, suitable for large-scale glacial lake hazard zonation. Details of this can be inferred from section 1 of the supplementary text.

4.7. Benefit of various data integration methods, especially AHP

In the weightage-based approach to assess GLOF hazard, we can design layers that are most suitable based on the knowledge and expertise, making this method particularly effective for regional-scale assessments. In such methods, priority should first be given to the most important parameter; here, population density was given higher weightage, followed by high-value infrastructure, such as hydropower plants. This is because these are most likely to be severely impacted, especially because they are located within 20–50 km downstream of a critical lake. The next priority should be the potential flood volume and the density of critical lakes. These factors significantly increase the likelihood of a GLOF occurring and its potential impact. Finally, the last parameters to consider in the weighting process are the road and railway networks, which often follow river channels and are thus highly susceptible to flood damage. In the hilly terrain, most settlements are located in a valley region, close to the river channel, making them prone to flooding. Thus, field-based data (discharge and river cross-sections) and flood hydrodynamic modelling are required for small-scale hazard and intensity mapping; therefore, settlements should be prioritised over roads and railways in the risk assessment of GLOF.

Advantages of AHP-Based GLOF hazard Assessment include: (i) Structured Decision Making: AHP provides a clear and systematic way to break down complex hazard assessments into manageable components. (ii) Expert judgement: the method leverages expert opinions to quantify the importance of various risk factors, making it adaptable to different regions and conditions. (iii) Integration of multiple data sources: AHP allows for the integration of diverse types of data (e.g. satellite imagery, field measurements, historical records) to create a comprehensive risk assessment. (iv) Prioritisation: it

produces a ranked list of glacial lakes, which is useful for decision-makers in allocating resources for GLOF risk management.

Limitations of this AHP method includes: (i) subjectivity: the pairwise comparisons rely on expert judgement, which may introduce subjectivity into the risk assessment, (ii) time-consuming: the method can be time-intensive, especially when dealing with a large number of criteria and sub-criteria, (iii) requires consistent data: the reliability of the results depends on the quality and consistency of the available data.

4.8. Climate change and glacial hazards

Global warming in the high-altitude regions of the Himalayas has become a pressing environmental concern, as rising temperatures are accelerating glacier retreat and altering the delicate cryospheric balance. Anthropogenic activities such as rapid urbanisation, deforestation, infrastructure development, and the emission of greenhouse gases have intensified the warming trend, leading to enhanced melting of snow and ice. This accelerated glacier retreat not only reduces long-term water availability but also increases the formation and expansion of unstable glacial lakes. As a consequence, the region faces heightened risks of natural hazards such as glacial lake outburst floods (GLOFs), debris flows, and flash floods. These cascading hazards pose serious threats to downstream communities, infrastructure, and ecosystems, emphasising the urgent need for climate-resilient planning and sustainable management practices in the Himalayan region. Rising temperatures have been responsible for the accelerated rate of growth of glacial lakes in the Himalayas. Studies conducted in Western Himalayas and Eastern Himalayas have conclusively shown that some glacial lakes (i.e. whose catchments have been classified as critical in this study) are expected to reach their maximum extent within the next 30 years under RCP 8.5, SSP2-4.5 and SSP5-8.5 climate scenarios (e.g. Gantayat and Ramsankaran 2023; Gantayat et al., 2024).

In recent years, glacial lake outburst floods (GLOFs), flash floods, and debris flow events have become significant concerns across various sectors of the Himalayan region. Extreme rainfall events exhibit a direct correlation with the occurrence of debris flows and flash floods, whereas rising temperatures often exhibit a lagged influence, contributing to GLOFs and related mass movement processes over time. Notable examples include the South Lhonak Lake outburst in 2023, Birendra Lake outburst in 2024, Meru debris flow in 2017 and 2024, the 2021 Chamoli disaster, and the Dharali debris flow in 2025 all of which can be attributed to rising temperatures and extreme precipitation events.

However, we did not attempt to include climate factors in our analyses because, as noted by Veh et al. (2022) and Harrison (2018), increasing global warming does not necessarily lead to an increase in the frequency of GLOF occurrences. Additionally, Himachal Pradesh experiences 3–4 flash flood incidents annually, primarily driven by climatic variability. Given the increasing occurrence of such events, comprehensive hazard assessment and mitigation studies are urgently required across the Himalayan terrain to minimise their adverse impacts on the environment and local communities.

5. Conclusions

In this study, we located ~221 critical lakes in the Himalaya. The critical lake density of the Kosi River basin and the Yarlung Zangbo basin were among the highest (i.e. ~47 and 22, respectively). For these lakes, we also estimated the distribution of lake count, area, and the corresponding hazard assessment pertaining to GLOF. At the basin scale, our extensive hazard assessment highlights several critical regions within the Himalayas that exhibit elevated susceptibility to glacial lake outburst flood (GLOF) hazards. The Chenab and Jhelum Basins in Kashmir, the Chenab and Beas Basins in Himachal Pradesh, the Koshi, Tama-Kosi, and Dudh-Kosi Basins in Nepal, the Kuri Chu sub-basin of the Manas Basin in Bhutan, and the Teesta Basin in Sikkim emerge as high-priority areas based on the integrated hazard index. These basins, characterised by a combination of high critical lake density, substantial probable flood volumes, and significant exposure of population and infrastructure, demand careful, site-specific hazard investigation prior to the establishment of human settlements, hydropower projects, and other costly infrastructure developments. When compared to the most comprehensive GLOF inventory of the Himalayas from 1533 CE to 2024 CE, more than 72% of the events were found to have occurred in lake basins whose hazard

assessment (i.e. as per this study) was classified as being at very high risk and high risk, respectively. In addition to that, <0.4% of the recorded GLOF events were found to be located in the lake basins (i.e. as per this study) that were categorised to be at Low risk. This is the first-ever regional assessment of GLOF hazards conducted for the entire Himalayan range. Across all sensitivity scenarios, our analyses showed that hazard assessment is most sensitive to population density, followed by critical lake count, while building and road densities remain the least sensitive parameters. Focused risk reduction and monitoring strategies should be prioritised within these basins to mitigate potential future GLOF-related disasters.

Acknowledgements

The work is partially financed by USDMA and WIHG, Dehradun. The authors would like to express their sincere gratitude to Dr. Ashim Sattar for his valuable insights, constructive suggestions, and contributions toward refining and improving the quality of this work. I want to give my special thanks to Mr. Sourav Anand and Mr. Shivyank Negi for helping me create the database. I would also like to thank IIT Kharagpur. For further data access, the corresponding authors can be contacted.

Litan Kumar Mohanty: writing – original draft, visualisation, validation, software, methodology, investigation, formal analysis, data curation, conceptualisation. Prateek Gantayat: editing, visualisation, and data validation.

Declaration of competing interest

The authors declare that they have no known competing financial interests or personal relationships that could have appeared to influence the work reported in this paper.

Disclosure statement

No potential conflict of interest was reported by the author(s).

Funding

No funding was received for this research.

Data availability statement

Data can be accessed upon request by contacting the corresponding author via email.

Author contributions

CRediT: **Litan Mohanty:** Conceptualization, Data curation, Formal analysis, Funding acquisition, Investigation, Methodology, Project administration, Resources, Software, Supervision, Validation, Visualization, Writing – original draft, Writing – review & editing; **Prateek Gantayat:** Supervision, Validation, Visualization, Writing – review & editing.

References

Aggarwal S, Rai SC, Thakur PK, Emmer A. 2017. Inventory and recently increasing GLOF susceptibility of glacial lakes in sikkim, eastern himalaya. Geomo. 295:39–54. https://doi.org/10.1016/j.geomorph.2017.06.014

Allen SK, Zhang G, Wang W, Yao T, Bolch T. 2019. Potentially dangerous glacial lakes across the Tibetan plateau revealed using a large-scale automated assessment approach. Sci Bull. 64(7):435–445. https://doi.org/10.1016/j.scib.2019.03.011

Allen SK et al. 2016. Glacial lake outburst flood risk in himachal pradesh, India: an integrative and anticipatory approach considering current and future threats. Nat Hazards. 84:1741–1763. https://doi.org/10.1007/s11069-016-2511-x

Armstrong WH, Anderson RS, Allen J, Rajaram H. 2016. Modeling the WorldView-derived seasonal velocity evolution of kennicott glacier, Alaska. J Glaciol. 62(234):763–777. https://doi.org/10.1017/jog.2016.66

Bajracharya SR. 2009. Glacial lake outburst floods risk reduction activities in Nepal. In: Asia-pacific symposium on new technologies for prediction and mitigation of sediment disasters. In: Asia-Pacific Symposium on New Technologies for Prediction and Mitigation of Sediment Disasters. Japan Society of Erosion Control Engineering (JSECE): Tokyo (Japan).

Bajracharya SR et al. 2020. Inventory of glacial lakes and identification of potentially dangerous glacial lakes in the Koshi, Gandaki, and Karnali River Basins of Nepal, the Tibet Autonomous Region of China. International Centre for Integrated Mountain Development (ICIMOD): Kathmandu (Nepal).

Banerjee A et al. 2024. Glacier retreat and lake outburst floods in the central himalayan region from 2000 to 2022. Nat Hazards. 120(6):5485–5508. https://doi.org/10.1007/s11069-024-06415-5
Banerjee A et al. 2025. Glacier and glacial lake dynamics from 1990 to 2024 and their impact on flood hazard in the central Nepal himalaya. J Mt Sci. 22(6):1926–1943. https://doi.org/10.1007/s11629-024-9298-0
Bhambri R et al. 2023. Heterogeneity in glacier thinning and slowdown of ice movement in the garhwal himalaya, India. Sci Total Environ. 875:162625. https://doi.org/10.1016/j.scitotenv.2023.162625
Bolch T et al. 2012. The state and fate of himalayan glaciers. Science. 336(6079):310–314.
Bolch T, Buchroithner MF, Peters J, Baessler M, Bajracharya S. 2008. Identification of glacier motion and potentially dangerous glacial lakes in the mt. Everest region/Nepal using spaceborne imagery. Nat Hazards Earth Syst Sci. 8(6):1329–1340. https://doi.org/10.5194/nhess-8-1329-2008
Bookhagen B, Burbank DW. 2006. Topography, relief, and TRMM-derived rainfall variations along the himalaya. Geophys Res Lett. 33(8):L08405.
Carrivick JL, Tweed FS. 2016. A global assessment of the societal impacts of glacier outburst floods. Glob Planet Change. 144:1–16. https://doi.org/10.1016/j.gloplacha.2016.07.001
Cook SJ, Quincey DJ. 2015. Estimating the volume of alpine glacial lakes. Earth Surf Dynam. 3(4):559–575. https://doi.org/10.5194/esurf-3-559-2015
Dubey S, Goyal MK. 2020. Glacial lake outburst flood hazard, downstream impact, and risk over the Indian Himalayas. Water Resour Res. 56(4):e2019WR026533. https://doi.org/10.1029/2019WR026533
Fujita K, et al. 2013. Potential flood volume of himalayan glacial lakes. Nat Hazards Earth Syst Sci. 13(7):1827–1839. https://doi.org/10.5194/nhess-13-1827-2013
Furian W, Loibl D, Schneider C. 2021. Future glacial lakes in high mountain Asia: an inventory and assessment of hazard potential from surrounding slopes. J Glaciol. 67(264):653–670. https://doi.org/10.1017/jog.2021.18
Gantayat P, Ramsankaran RAAJ. 2023. Modelling evolution of a large, glacier-fed lake in the Western Indian himalaya. Sci Rep. 13(1):1840. https://doi.org/10.1038/s41598-023-28144-8
Gantayat P, Sattar A, Haritashya UK, Ramsankaran RAAJ, Kargel JS. 2024. Evolution of the lower barun lake and its exposure to potential mass movement slopes in the Nepal himalaya. Sci Total Environ. 949:175028. https://doi.org/10.1016/j.scitotenv.2024.175028
Harrison S, et al. 2018. Climate change and the global pattern of moraine-dammed glacial lake outburst floods. Cryosphere. 12(4):1195–1209. https://doi.org/10.5194/tc-12-1195-2018
Hirabayashi Y, et al. 2013. Global flood risk under climate change. Nat Clim Change. 3(9):816–821. https://doi.org/10.1038/nclimate1911
Huggel C. 2004. Assessment of glacial hazards based on remote sensing and GIS modeling. Phys Geogr Ser. 44.
Huggel C, Kääb A, Salzmann N. 2006. Evaluation of QuickBird and IKONOS imagery for assessment of high-mountain hazards. EARSeL eProc. 5(1):51–62.
IPCC. 2014. Summary for policymakers. In: Field CB, editor. Climate Change 2014: Impacts, Adaptation, and Vulnerability. Part A: Global and Sectoral Aspects. Contribution of Working Group II to the Fifth Assessment Report of the Intergovernmental Panel on Climate Change. Cambridge University Press: Cambridge (UK) and New York (NY):. p 1–32.
Kääb A, Reichmuth T. 2005. Advance mechanisms of rock glaciers. Permafr Periglac Process. 16(2):187–193. https://doi.org/10.1002/ppp.507
Khadka N, Zheng G, Chen X, Zhong Y, Allen S K, Gouli M R et al. 2024. An ice-snow avalanche triggered small glacial lake outburst flood in birendra lake, Nepal himalaya. Nat Hazards. 121(5):6357–6365.
Komori J, Koike T, Yamanokuchi T, Tshering P. 2012. Glacial lake outburst events in the Bhutan Himalayas. Glob Environ Res. 16(1):59–70.
Lützow N, Veh G, Korup O. 2023. A global database of historic glacier lake outburst floods. Earth Syst Sci Data Discuss. 2023:1–27. 15:2983–3000. https://doi.org/10.5194/essd-15-2983-2023
Maurer JM et al. 2020. Seismic observations, numerical modeling, and geomorphic analysis of a glacier lake outburst flood in the Himalayas. Sci Adv. 6(38):eaba3645. https://doi.org/10.1126/sciadv.aba3645
McKillop RJ, Clague JJ. 2007. Statistical, remote sensing-based approach for estimating the probability of catastrophic drainage from moraine-dammed lakes in southwestern British Columbia. Glob Planet Change. 56(1-2):153–171. https://doi.org/10.1016/j.gloplacha.2006.07.004
Mohanty LK, Maiti S. 2021a. Regional morphodynamics of supraglacial lakes in the everest himalaya. Sci Total Environ. 751:141586. https://doi.org/10.1016/j.scitotenv.2020.141586
Mohanty L, Maiti S. 2021b. Probability of glacial lake outburst flooding in the himalaya. Resour Environ Sustain. 5:100031. https://doi.org/10.1016/j.resenv.2021.100031
Mohanty L, Maiti S. 2024. A GIS and remote sensing-based approach on supraglacial lake dynamics study in the himalayan glaciers. J Geol Soc India. 100(10):1457–1465. https://doi.org/10.17491/jgsi/2024/174000
Mohanty L, Maiti S, Dixit A. 2023a. Spatio-temporal assessment of regional scale evolution and distribution of glacial lakes in himalaya. Front Earth Sci. 10:1038777. https://doi.org/10.3389/feart.2022.1038777
Mohanty L, Pateswary V, Maiti S, Mohanty DD. 2023b. Future prediction of existing glacial lake's size in the himalaya by Markov model and glacial surface topography. All Earth. 35(1):329–343. https://doi.org/10.1080/27669645.2023.2256034

Mondal SK et al. 2025. Glacial lakes outburst susceptibility and risk in the eastern Himalayas using analytical hierarchy process and backpropagation neural network models. Geom Nat Hazards Risk. 16(1):2449134. https://doi.org/10.1080/19475705.2024.2449134
Mondal SK, Bharti R. 2022. Glacial burst triggered by triangular wedge collapse: a study from trisul mountain near ronti glacier valley. Geom Nat Hazards Risk. 13(1):830–853.
Mondal SK, Patel VD, Bharti R, Singh RP. 2023. Causes and effects of shisper glacial lake outburst flood event in Karakoram in 2022. Geom Nat Hazards Risk. 14(1):2264460. https://doi.org/10.1080/19475705.2023.2264460
Nie Y, Liu W, Liu Q, Hu X, Westoby MJ. 2020. Reconstructing the chongbaxia tsho glacial lake outburst flood in the eastern himalaya: evolution, process and impacts. Geomorphology. 370:107393. https://doi.org/10.1016/j.geomorph.2020.107393
Nie Y et al. 2018. An inventory of historical glacial lake outburst floods in the Himalayas based on remote sensing observations and geomorphological analysis. Geomorphology. 308:91–106. https://doi.org/10.1016/j.geomorph.2018.02.002
Nikitin AM. 1987. Lakes of Central Asia. Gidrometeoizdat: Leningrad (RU). p 106.
Pandey A et al. 2024. Spatiotemporal snowline status and climate variability impact assessment: a case study of pindari river basin, kumaun himalaya, India. Environ Sci Eur. 36(1):104. https://doi.org/10.1186/s12302-024-00924-7
Pelto M, Network WGMS. 2020. Alpine glaciers. Bull Am Meteorol Soc. 101(8):S37–S38.
Quincey DJ et al. 2007. Early recognition of glacial lake hazards in the himalaya using remote sensing datasets. Glob Planet Change. 56(1-2):137–152. https://doi.org/10.1016/j.gloplacha.2006.07.013
Redpath TAN, Sirguey P, Fitzsimons SJ, Kääb A. 2013. Accuracy assessment for mapping glacier flow velocity and detecting flow dynamics from ASTER satellite imagery: tasman glacier, New Zealand. Remote Sens Environ. 133:90–101. https://doi.org/10.1016/j.rse.2013.02.008
Rubatto D, Chakraborty S, Dasgupta S. 2013. Timescales of crustal melting in the higher himalayan crystallines (Sikkim, Eastern Himalaya) inferred from trace element-constrained monazite and zircon chronology. Contrib Mineral Petrol. 165:349–372. https://doi.org/10.1007/s00410-012-0812-y
Sattar A, Haritashya U K, Kargel J S, Karki A. 2022. Transition of a small Himalayan glacier lake outburst flood to a giant transborder flood and debris flow. Scientific Report. 12(1):12421.
Sattar A et al. 2025. The sikkim flood of October 2023: drivers, causes, and impacts of a multihazard cascade. Science. 387(6740):eads2659.
Song, C., Sheng, Y., Wang, J., Ke, L., Madson, A., & Nie, Y. 2017. Heterogeneous glacial lake changes and links of lake expansions to the rapid thinning of adjacent glacier termini in the Himalayas. Geomorphology. 280:30–38.
Song, C., Huang, B., Richards, K., Ke, L., & Hien Phan, V. 2014. Accelerated lake expansion on the Tibetan Plateau in the 2000s: Induced by glacial melting or other processes? *Water Resources Research*. 50(4):3170-31863170–3186.
Schwanghart W, Worni R, Huggel C, Stoffel M, Korup O. 2016. Uncertainty in the himalayan energy–water nexus: estimating regional exposure to glacial lake outburst floods. Environ Res Lett. 11(7):074005. https://doi.org/10.1088/1748-9326/11/7/074005
Shijin W, Dahe Q, Cunde X. 2015. Moraine-dammed lake distribution and outburst flood risk in the Chinese himalaya. J Glaciol. 61(225):115–126. https://doi.org/10.3189/2015JoG14J097
Shrestha F et al. 2023. A comprehensive and version-controlled database of glacial lake outburst floods in high mountain Asia. Earth Syst Sci Data. 15(9):3941–3961. https://doi.org/10.5194/essd-15-3941-2023
Shrestha AB et al. 2010. Glacial lake outburst flood risk assessment of sun koshi basin, Nepal. Geomatics Nat Hazards Risk. 1(2):157–169. https://doi.org/10.1080/19475701003668968
Shugar DH et al. 2020. Rapid worldwide growth of glacial lakes since 1990. Nat Clim Change. 10(10):939–945. https://doi.org/10.1038/s41558-020-0855-4
Shugar DH et al. 2021. A massive rock and ice avalanche caused the 2021 disaster at chamoli, Indian himalaya. Sci. 373(6552):300–306.
Taylor C, Robinson TR, Dunning S, Carr JR, Westoby MJ. 2023. Glacial lake outburst floods threaten millions globally. Nat Commun. 14(1):487. https://doi.org/10.1038/s41467-023-36033-x
Uyan M. 2013. GIS-based solar farms site selection using analytic hierarchy process (AHP) in karapinar region, Konya/Turkey. Renew Sustain Energy Rev. 28:11–17. https://doi.org/10.1016/j.rser.2013.07.042
Veh G et al. 2022. Trends, breaks, and biases in the frequency of reported glacier lake outburst floods. Earths Future. 10(3):e2021EF002426.
Wang X et al. 2013. Changes of glacial lakes and implications in Tian Shan, Central Asia, based on remote sensing data from 1990 to 2010. Environ Res Lett. 8(4):044052. https://doi.org/10.1088/1748-9326/8/4/044052
Wang S, Che Y, Xinggang M. 2020. Integrated risk assessment of glacier lake outburst flood (GLOF) disaster over the Qinghai–Tibetan plateau (QTP). Landslides. 17:2849–2863. https://doi.org/10.1007/s10346-020-01443-1
Wangchuk S, Bolch T. 2020. Mapping of glacial lakes using Sentinel-1 and Sentinel-2 data and a random forest classifier: strengths and challenges. Sci Remote Sens. 2:100008. https://doi.org/10.1016/j.srs.2020.100008
Washakh RMA et al. 2019. GLOF risk assessment model in the Himalayas: a case study of a hydropower project in the upper arun river. Water. 11(9):1839. https://doi.org/10.3390/w11091839
Wijngaard RR, et al. 2017. Future changes in hydro-climatic extremes in the upper Indus, Ganges, and Brahmaputra river basins. PLoS One. 12(12):e0190224. https://doi.org/10.1371/journal.pone.0190224
Yu Y, Li B, Li Y, Jiang W. 2024. Retrospective analysis of glacial lake outburst flood (GLOF) using AI earth InSAR and optical images: a case study of south lhonak lake, sikkim. Remote Sens. 16(13):2307. https://doi.org/10.3390/rs16132307

Zhang G et al. 2023. Underestimated mass loss from lake-terminating glaciers in the greater himalaya. Nat Geosci. 16(4):333–338. https://doi.org/10.1038/s41561-023-01150-1

Zhang T, Wang W, An B. 2024. A massive lateral moraine collapse triggered the 2023 south lhonak lake outburst flood, sikkim Himalayas. Landslides. 1:13.

Zhang G, Yao T, Xie H, Wang W, Yang W. 2015. An inventory of glacial lakes in the third pole region and their changes in response to global warming. Glob Planet Change. 131:148–157. https://doi.org/10.1016/j.gloplacha.2015.05.013